Performance improvement of flexible robot using combined observer-controller and particle swarm optimization

Fouad Haouari[1,*], Nourdine Bali[2], Mohamed Tadjine[1], Mohamed Seghir Boucherit[1]

1. Department of Electrical Engineering, Process Control Laboratory, ENP 10 Avenue Hassan Badi P.O Box 182 Algiers, 16200, Algeria

2. Electrical Engineering and Computing Faculty, USTHB P.O Box 32 El Alia, Bab Ezzouar Algiers, 16111, Algeria

haouai_fouad@yahoo.fr

ABSTRACT. The aim of this study is to examine the robust control design based on coefficient diagram method with backstepping control combined with an observer for position control of the flexible joint manipulator. A simulation model with stability analysis was established where the parameters of the observer-controller are tuned by means of particle swarm optimization. Through this study, it was found that the proposed control scheme is effective, and the results indicate that ours approach ensures the asymptotic convergence of the actual joints positions to theirs desired trajectory, and robustness where the system is subjected to external disturbance and parameters uncertainties.

RÉSUMÉ. Le but de cette étude est d'examiner la conception de contrôle robuste basée sur la méthode du diagramme de coefficients avec contrôle de la rétrogradation associé à un observateur pour le contrôle de la position du manipulateur joint flexible. Un modèle de simulation avec analyse de stabilité a été établi où les paramètres de l'observateur-contrôleur sont réglés au moyen de l'optimisation par essaims particulaires. Cette étude a montré que le schéma de contrôle proposé est efficace et les résultats indiquent que notre approche garantit la convergence asymptotique des positions articulaires actuelles vers la trajectoire souhaitée et une robustesse se présente lorsque le système est soumis à des perturbations externes et à des incertitudes sur les paramètres.

KEYWORDS: flexible robot, backstepping control, coefficient diagram method, nonlinear observer, particle swarm optimization.

MOTS-CLÉS: robot flexible, control par backstepping, méthode de diagramme des coefficients, observateur non linéaire, optimisation par essaim de particule.

DOI:10.3166/JESA.50.485-505 © 2017 Lavoisier

1. Introduction

Flexible robot manipulators are widely used in industrial and space applications and enhances safety for service robots which interact directly with human bodies, the robust control problem of flexible robot becomes more complicated then rigid manipulator, many difficulties in flexible manipulators are also overcome hardly, such as high nonlinearity, elastic deformation and various uncertainties (Ali *et al.*, 2014). Various methods are established to design effective control of flexible joint manipulator such as fuzzy PID control (Yen *et al.*, 2012), sliding mode tracking control and the robust control. The major limitation of these control method is that they require state measurement; nevertheless, in order to apply advanced concepts of control in flexible joint, the acquaintance of state variables is not usually available. This can be realised by means of state observers. Newly, a significant research activity has been dedicated to this kind of nonlinear systems observation.

Backstepping controller (Sabiri, 2016; Benzineb, 2012) is the most frequently employed technique for controlling nonlinear systems and is very efficient but its performance depends on the nonlinear system modelling. The real systems are exposed to variation with time, so the equations used to model them can vary. As a result, the performance of classical backstepping controller can get worse. An improvement in controller, by introducing coefficient diagram method CDM algorithm (Mohamed, 2016; Mitsantisuk, 2013) can solve this problem. The resulting controller (CDM-backstepping) is used with nonlinear observer (Khan, 2016; Furtat, 2016) to control a class of flexible joint robotic manipulators; this method of control assures recursively the globally asymptotic stabilizing controls by corresponding Lyapunov functions for subsystems.

The use of optimization algorithms as alternative methods for tuning parameters of controllers has been a modern subject of research in systems control. If the optimization problem is convex, the overall minimum is assured. Conversely, for non-convex problems, there is no possibility of a global solution. In this context, particle swarm optimization **(**PSO) (Yushu, 2013; Hassani, 2016) can be used in order to find an optimal solution of problems considering simple trial operations, but good enough for enhancing the performance of the system when the controller can be designed and validated considering the system model via simulation.

The paper is organised as follows. In the second section, two joints flexible manipulator state space model is presented. In the third section a brief description of the CDM controller for linear system. In the fourth section, the stability analysis of the closed loop system based on observer and CDM-backstepping is developed. In the fifth section PSO is briefly described. Then, optimum values of parameters control are obtained. In the sixth section, presents the simulation results and finally, the seventh section concludes the paper.

2. Robot dynamic and state space model

The equations of motion of two joints flexible robot can be described as (Yen *et *al.*, 2012).

$$\begin{cases} M(q)\ddot{q}+C(q,\dot{q})\dot{q}+G(q)=K_s(\theta-q) \\ J\ddot{\theta}+B_a\dot{\theta}-K_s(q-\theta)=\tau \end{cases} \tag{1}$$

$q=\begin{bmatrix} q_1 & q_2 \end{bmatrix}^T$, $\theta=\begin{bmatrix} \theta_1 & \theta_2 \end{bmatrix}^T$, $K_s=diag\left(K_{s1},\ K_{s2}\right)$, $J=diag\left(J_1,\ J_2\right)$,

$\tau=\begin{bmatrix} \tau_1 & \tau_2 \end{bmatrix}^T$, $G(q)=\begin{bmatrix} g_1 & g_2 \end{bmatrix}^T$, $B_a=diag\left(B_{a1},\ B_{a2}\right)$,

$C(q,\dot{q})=-\beta diag(\dot{q}_2,\dot{q}_1)$, $M(q)=\begin{bmatrix} \alpha_1 & \alpha_2 \\ \alpha_2 & \alpha_3 \end{bmatrix}$.

$\alpha_1=(m_1+m_2)l_1^2$, $\alpha_2=m_2l_1l_2\left(\sin(q_1)\sin(q_2)+\cos(q_1)\cos(q_2)\right)$, $\alpha_3=m_2l_2^2$,

$g_2=-m_2l_2g\sin(q_2)$, $\beta=m_2l_1l_2\left(\cos(q_1)\sin(q_2)-\sin(q_1)\cos(q_2)\right)$,

$g_1=-(m_1+m_2)l_1g\sin(q_1)$.

Let $x=\left[x_1,\cdots,\ x_8\right]=\left[q_1,\ \dot{q}_1,\ \theta_1,\ \dot{\theta}_1,\ q_2,\ \dot{q}_2,\ \theta_2,\ \dot{\theta}_2\right]$

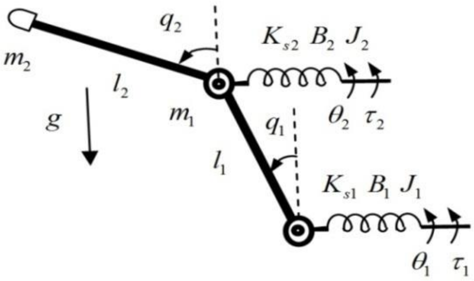

Figure 1. Two joints flexible manipulator

The state space model of two joints flexible manipulator which is shown in Figure 1 can be represented as next formula:

$$\begin{cases} \dot{x}_1=x_2,\ \dot{x}_2=F_{11}(x),\ \dot{x}_3=x_4 \\ \dot{x}_4=F_{12}(x)+\left(1/J_1\right)\tau_1 \\ \dot{x}_5=x_6,\ \dot{x}_6=F_{21}(x),\ \dot{x}_7=x_8 \\ \dot{x}_8=F_{22}(x)+\left(1/J_2\right)\tau_2 \\ y=\begin{bmatrix} x_1 & x_5 \end{bmatrix}^T \end{cases} \tag{2}$$

Where

$$F_{22}(x) = \frac{K_{s2}}{J_2}x_5 - \frac{K_{s2}}{J_2}x_7 - \frac{B_{a2}}{J_2}x_8\,,\ F_{12}(x) = \frac{K_{s1}}{J_1}x_1 - \frac{K_{s1}}{J_1}x_3 - \frac{B_{a1}}{J_1}x_4\,,$$

$$F_{21}(x) = \frac{\alpha_2 g_1 - \alpha_1 g_2}{\alpha_2^2 - \alpha_1\alpha_3}\ ,\ F_{11}(x) = \frac{\alpha_3 g_1 - \alpha_2 g_2}{\alpha_1\alpha_3 - \alpha_2^2}\,.$$

3. Robot dynamic and state space model

CDM is a recent polynomial representation to create control systems with the lowest degree and can guaranties the stability and robustness without overshoot and with a preferred desired time response.

The output of system to be controlled by CDM is represented as follows

$$y_e = \frac{N(s)F(s)}{P(s)}r_e + \frac{A(s)N(s)}{P(s)}d_e \tag{3}$$

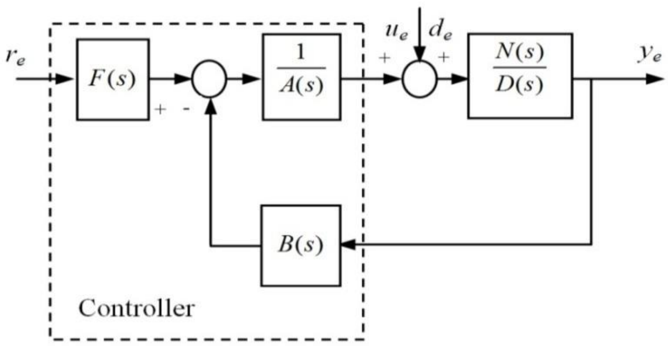

Figure 2. Block scheme of the CDM control

The standard single input single output block scheme of the CDM control is exposed in Figure 2, *P(s)* is formulated as (Mohamed, 2015; Bernard, 2014).

$$P(s) = D(s)A(s) + N(s)B(s) = \sum_{i=0}^{n}\mu_i s^i = \mu_0\left[\{\sum_{i=2}^{n}(\prod_{j=1}^{i-1}\frac{1}{\gamma_{i-j}^{j}})(T_0 s)^i\} + T_0 s + 1\right] \tag{4}$$

Where

$$N(s) = a_m s^m + .. + a_0\,,\ D(s) = b_n s^n + ...b_0\,, A(s) = \sum_{i=0}^{n} l_i s^i \text{ and } B(s) = \sum_{i=0}^{n} k_i s^i\,.$$

The key parameters, $T_0=\mu_1/\mu_0$ indicate the speed of system response in closed loop, however, the constants $\gamma_i = \mu_i^2 / (\mu_{i-1}\mu_{i+1})$ and $\gamma_i^* = 1/\gamma_{i-1} + 1/\gamma_{i+1}$, $i \in [1, n-1]$ are indicative of stability and the shape of the time response, on the other hand, the variation of stability indices assure the robustness in the presence of the perturbations and parameters variations. The constants t_s and T_0 can be set as $T_0 = t_s/(2.5 \sim 3)$ with $\gamma_1 = 2.5$, $\gamma_i = 2$, $\gamma_0 = \gamma_n = \infty$, $i = 2 \sim (n-1)$.

The values of γ_i prearranged for the standard form can be adjusted to provide the needed performance to provide the needed performance, so that $\gamma_i>1.5\gamma_i^*$ for all $i=1\sim(n-1)$.

The polynomial $F(s)=P(s)|_{s=0}/N(s)$ is used to reduce the steady state error.

4. Stability analysis of the control system

The CDM-backstepping approach provides a methodical and recursive algorithm that combines the choice of a Lyapunov function with the design of a controller (Chen, 2016; Zhou, 2016). The most appealing point of it is to use the virtual control variable (Ba, 2016; Wang, 2016) to make the original high order system to be simple enough, thus the final control outputs can be derived step by step through suitable Lyapunov positive definite functions as shown in Fig 3, all nonlinearities can be cancelled by the actual control (Chang, 2010; Bossoufi, 2015).

This part deals with the angular positions control by means of the proposed combined observer-controller of flexible manipulator whish considered a Lipschitz system by using Lyapunov function in four steps, which yields external disturbance parametric variation and noise rejections.

The state space model given by equation (2) can be formulated as follows

$$\begin{cases} \dot{x} = Ax + F(x) + Bu \\ y = Cx \end{cases} \tag{5}$$

With the matrices $A = diag(A_1, A_3)$, $B = \begin{bmatrix} B_1 & B_2 \end{bmatrix}^T$,

$$A_1 = \begin{bmatrix} 0 & 1 & 0 & 0 \\ 0 & 0 & 0 & 0 \\ 0 & 0 & 0 & 1 \\ \frac{K_{s1}}{J_1} & 0 & -\frac{K_{s1}}{J_1} & -\frac{B_{a1}}{J_1} \end{bmatrix}, \quad A_3 = \begin{bmatrix} 0 & 1 & 0 & 0 \\ 0 & 0 & 0 & 0 \\ 0 & 0 & 0 & 1 \\ \frac{K_{s2}}{J_2} & 0 & -\frac{K_{s2}}{J_2} & -\frac{B_{a2}}{J_2} \end{bmatrix}, \quad B_1 = \begin{bmatrix} 0 & 0 \\ 0 & 0 \\ 0 & 0 \\ \frac{1}{J_1} & 0 \end{bmatrix},$$

$$C = \begin{bmatrix} 1 & 0 & 0 & 0 & 0 & 0 & 0 & 0 \\ 0 & 0 & 0 & 0 & 1 & 0 & 0 & 0 \end{bmatrix}, \quad B_2^T = \begin{bmatrix} 0 & 0 & 0 & 1/J_2 \\ 0 & 0 & 0 & 0 \end{bmatrix}$$

and $F(x)=\begin{bmatrix}0 & F_{11}(x) & 0 & 0 & 0 & F_{21}(x) & 0 & 0\end{bmatrix}^T$.

To propose the state observer, the Lipschitz condition on the vector of nonlinear function *F(x)* with respect to *x* must be guaranteed, such that $\left\|F(x)\text{-}F(\hat{x})\right\| \le \kappa \left\|x - \hat{x}\right\|$.

The state-observer of the considered system given by (2) will be assumed to be of the next form

$$\begin{cases}\dot{\hat{x}} = A\hat{x} + F(\hat{x}) + Bu + \psi(y-\hat{y}) \\ \hat{y} = C\hat{x}.\end{cases} \tag{6}$$

Where the matrix ψ is given by

$$\psi = \begin{bmatrix} h_{11} & h_{12} \\ \vdots & \vdots \\ h_{81} & h_{82}\end{bmatrix} \tag{7}$$

Then defining the error $E_o = x - \hat{x}$ consequently, its dynamics is given as

$$\dot{E}_o = (A-\psi C)E_o + F(x) - F(\hat{x}) = A_o E_o + F(x) - F(\hat{x}) \tag{8}$$

We can calculate the matrix gain ψ if the pair (A, C) is detectable (Khan *et al.*, 2016) and $A_o = (A-\psi C)$ is Hurwitz (Furtat and Tupichin, 2016), in this case there are two symmetric positive definite matrices *P* and *Q* so as to verify the equality $A_0^T P + PA_0 = -Q$.

Consider the Lyapunov function candidate $V_o = e_o^T P e_o$, its time derivative is

$$\begin{aligned}\dot{V}_o &= E_o{}^T(A_o{}^T P + PA_o)E_o + 2E_o{}^T P\left(F(x) - F(\hat{x})\right) = -E_o{}^T Q E_o \\ &+2E_o{}^T P\left(F(x)-F(\hat{x})\right) \le -\left(\varsigma_{\min}(Q) - 2\chi\left\|P\right\|\right)\left\|E_o\right\|^2 = -\omega\left\|E_o\right\|^2\end{aligned} \tag{9}$$

If we take $\omega = \left(\varsigma_{\min}(Q) - 2\chi\left\|P\right\|\right) > 0$, the asymptotic convergence of error E_o can be assured with $\dot{V}_o \le -\omega e_o^2 \le 0$.

Consider the correspondent nonlinear observer for system specified by equation (5) is as the following form

$$\begin{cases}\dot{\hat{x}} = A\hat{x} + F(x) + Bu + \psi(y-\hat{y}) \\ \hat{y} = C\hat{x}\end{cases} \tag{10}$$

In the first step, the first error is defined $Z_1 = \hat{X}_1 - X_d$, $\hat{X}_1 = \left[\hat{x}_1, \hat{x}_5\right]^T$ and $X_d = \left[x_{d1} \quad x_{d2}\right]^T$ Its time derivative is specified as $\dot{Z}_1 = \dot{X}_1 - \dot{X}_d = X_2 + \psi_1 E_{o1} - \dot{X}_d$ with $E_{o1} = X_1 - \hat{X}_1$, $\hat{X}_2 = \left[\hat{x}_2, \ \hat{x}_6\right]^T$ and $\psi_1 = \begin{bmatrix} h_{11} & h_{12} \\ h_{51} & h_{52} \end{bmatrix}$

The first candidate Lyapunov function is selected as

$$V_1 = 0.5 Z_1^T Z_1 + V_o \tag{11}$$

Differentiate to get $\dot{V}_1 = Z_1^T \dot{Z}_1 + \dot{V}_o$, then one has $\dot{V}_1 \le Z_1^T \dot{Z}_1 - \omega \left\| E_o \right\|^2 = Z_1^T \left(\hat{X}_2 + E_{o1} - \dot{X}_d \right) - \omega \left\| E_o \right\|^2$.

We now choose the first desired control input as $\varphi_1 = -\lambda_1 Z_1 + \dot{X}_d$ with $\lambda_1 > 0$, and $Z_2 = \hat{X}_2 - \varphi_1$, Differentiating to time the first Lyapunov function V_1 gives $\dot{V}_1 \le Z_1^T \left(Z_2 + E_{o1} - \dot{X}_d + \varphi_1 \right) - \omega \left\| E_o \right\|^2$.

Where the second error $E_{o2} = X_2 - \hat{X}_2$ and $\hat{X}_2$ is taken as control input. Then, the derivative of V_1 is

$$\dot{V}_1 \le -\lambda_1 Z_1^T Z_1 + Z_1^T Z_2 + Z_1^T \psi_1 E_{o1} - \omega \left\| E_o \right\|^2 \tag{12}$$

If we take in consideration the generic inequality $Z_1^T \psi_1 E_{o1} \le \kappa_1 Z_1^T Z_1 + \left(1/4\kappa_1\right) \left\| \psi_1 E_{o1} \right\|^2$, with $\kappa_1 > 0$, one has

$$\begin{aligned} \dot{V}_1 &\le Z_1^T Z_2 - (\lambda_1 - \kappa_1) Z_1^T Z_1 + \left(1/4\kappa_1\right) \left\| \psi_{o1} E_{o1} \right\| - \omega \left\| E_o \right\|^2 \\ &\le Z_1^T Z_2 - (\lambda_1 - \kappa_1) Z_1^T Z_1 - \left(\omega - (\left\| \psi_{o1} \right\|^2 / 4\kappa_1) \right) \left\| E_{o1} \right\|^2 \end{aligned}$$

If we take $\omega > \left\| \psi_{o1} \right\|^2 / 4\kappa_1$ and $\lambda_1 > \kappa_1$, with an appropriate choice of λ_1 and κ_1, we obtain $\dot{V}_1 \le -\bar{\lambda}_1 Z_1^T Z + Z_1^T Z_2, \quad \bar{\lambda}_1 > 0$.

The time derivative of Z_2 is given by

$$\dot{Z}_2 = \dot{\hat{X}}_2 - \dot{\varphi}_1 = F_1(\hat{X}) + \psi_2 E_{o1} - \dot{\varphi}_1 \tag{13}$$

with $\dot{\varphi}_1 = -\lambda_1 \dot{Z}_1 + \ddot{X}_d = -\lambda_1 \hat{X}_2 + \lambda_1 X_d + \ddot{X}_d$ and $\psi_2 = \begin{bmatrix} h_{21} & h_{22} \\ h_{61} & h_{62} \end{bmatrix}$.

Select the second Lyapunov function as $V_2 = V_1 + 0.5 Z_2^T Z_2 + V_o$, Its derivative is written as

$$\dot{V}_2 = \dot{V}_1 + Z_2^T \dot{Z}_2 + \dot{V}_o \leq -\bar{\lambda}_1 Z_1^T Z_1 + Z_1^T Z_2 + Z_2^T \dot{Z}_2 - \omega \|E_o\|^2 \quad (14)$$

Substituting equation (13) into (14) gives

$$\dot{V}_2 \leq -\bar{\lambda}_1 Z_1^T Z_1 + Z_1^T Z_2 + Z_2^T (F_1(\hat{x}) + \psi_2 E_{o1} - \dot{\varphi}_1) - \omega \|E_o\|^2 \quad (15)$$

Now, the desired control input φ_2 of $\hat{X}_3$ is chosen as $\varphi_2 = \hat{X}_3 - F_1(\hat{x}) - Z_1 - \bar{\lambda}_2 Z_2 + \dot{\varphi}_1$.

Defining the error $Z_3 = \hat{X}_3 - \varphi_2$, with $\hat{X}_3 = [\hat{x}_3, \hat{x}_7]^T$ substituting the term of φ_2 in equation (15), then $\dot{V}_2 \leq -\bar{\lambda}_1 Z_1^T Z_1 - \lambda_2 Z_2^T Z_2 + Z_2^T Z_3 + Z_2^T \psi_2 E_{o1} - \omega \|E_o\|^2$.

Exploiting the generic inequality $Z_2^T \psi_2 E_{o1} \leq \kappa_2 Z_2^T Z_2 + (1/4\kappa_2) \|\psi_2 E_{o1}\|^2$ with $\kappa_2 > 0$, the previous equation can be restructured as

$$\begin{aligned} \dot{V}_2 &\leq -\bar{\lambda}_1 Z_1^T Z_1 + Z_2^T Z_3 - (\lambda_2 - \kappa_2) Z_2^T Z_2 + (1/4\kappa_2) \|\psi_2 E_{o1}\|^2 - \omega \|E_o\|^2 \\ &= -\bar{\lambda}_1 Z_1^T Z_1 - \bar{\lambda}_2 Z_2^T Z_2 + Z_2^T Z_3 - \left(\omega - \|\psi_2\|^2 / 4\kappa_2\right) \|E_{o1}\|^2 \end{aligned} \quad (16)$$

Taking the constants $\omega > \|\psi_2\|^2 / 4\kappa_2$, $\lambda_2 > \kappa_2$ and $\bar{\lambda}_2 = \lambda_2 - \kappa_2$, then $\dot{V}_2 \leq -\bar{\lambda}_1 Z_1^T Z_1 - \bar{\lambda}_2 Z_2^T Z_2 + Z_2^T Z_3$.

After that, calculate the time derivative of Z_3, make available $\dot{Z}_3 = \dot{\hat{X}}_3 \text{-} \dot{\varphi}_2 = \dot{\hat{X}}_4 + \psi_3 E_{o1} - \dot{\varphi}_2$, where $\hat{X}_3 = [\hat{x}_3, \hat{x}_7]^T$ and $\psi_3 = \begin{bmatrix} h_{31} & h_{32} \\ h_{71} & h_{72} \end{bmatrix}$.

Taking the third Lyapunov function as follows $V_3 = V_2 + 0.5 Z_3^T Z_3 + V_o$, at that moment

$\dot{V}_3 \leq -\bar{\lambda}_1 Z_1^T Z_1 - \bar{\lambda}_2 Z_2^T Z_2 + Z_2^T Z_3 + Z_3^T \dot{Z}_3 + \dot{V}_o$, then

$$\dot{V}_3 \leq -\bar{\lambda}_1 Z_1^T Z_1 - \bar{\lambda}_2 Z_2^T Z_2 + Z_2^T Z_3 + Z_3^T (\dot{\hat{X}}_4 + \psi_3 E_{o1} - \dot{\varphi}_2) - \omega \|E_o\|^2 \quad (17)$$

Taking $\varphi_3 = Z_2 - \lambda_3 Z_3 + \dot{\varphi}_2$, in that case the time derivative of V_3 is given as

$$\dot{V}_3 \leq -\bar{\lambda}_1 Z_1^T Z_1 - \bar{\lambda}_2 Z_2^T Z_2 + Z_2^T Z_3 - \lambda_3 Z_3^T Z_3 + Z_3^T Z_4 + Z_3^T \psi_3 E_{o1} - \omega \|E_o\|^2 \quad (18)$$

With the law $Z_3^T \psi_2 E_{o1} \leq \kappa_3 Z_3^T Z_3 + (1/4\kappa_3) \|\psi_3 E_{o1}\|^2$ and $\kappa_3 > 0$, the last equation can be reorganized as

$$\dot{V}_3 \leq -\bar{\lambda}_1 Z_1^T Z_1 - \bar{\lambda}_2 Z_2^T Z_2 - \lambda_3 Z_3^T Z_3 + Z_3^T Z_4 + \kappa_3 Z_3^T Z_3 + (1/4\kappa_3) \|\psi_3 E_{o1}\|^2 - \omega \|E_o\|^2$$

As a result

$$\dot{V}_3 \le -\bar{\lambda}_1 Z_1^T Z_1 - \bar{\lambda}_2 Z_2^T Z_2 - (\lambda_3 - \kappa_3) Z_3^T Z_3 + Z_3^T Z_4 - (\omega - \|\psi_3\|^2 / 4\kappa_3) \|E_{o1}\|^2 \quad (19)$$

Taking

$\omega > \|\psi_{o3}\|^2 / 4\kappa_3$ and $\lambda_3 > \kappa_3$,and $\bar{\lambda}_3 = \lambda_3 - \kappa_3$, This provide $\dot{V}_2 \le -\bar{\lambda}_1 Z_1^T Z_1 - \bar{\lambda}_2 Z_2^T Z_2 - \bar{\lambda}_3 Z_3^T Z_3 + Z_3^T Z_4$.

Choose the final Lyapunov function as follows

$$V_4 = V_3 + 0.5 Z_4^T Z_4 + V_o \quad (20)$$

Define the desired control input φ_3 such that

$$Z_4 = \hat{X}_4 - \varphi_3 \quad (21)$$

Its derivative is expressed as $\dot{Z}_4 = \dot{\hat{X}}_4 - \dot{\varphi}_3$.

After that, one has $\dot{Z}_4 = F_2(\hat{X}) + \psi_4 E_{o1} - \dot{\varphi}_3$ with $F_2(\hat{X}) = \left[F_{12}(\hat{x}), F_{22}(\hat{x})\right]^T$.

Considering $\zeta = \hat{X}_4$ with $\hat{X}_4 = \left[\hat{x}_4, \hat{x}_8\right]^T$, this gives $\dot{\zeta} = G_1(\hat{X}) + G_2(\hat{X})u$ where $G_2(\hat{x}) = diag\left(a_4, a_8\right)$,

$G_1(\hat{x}) = F_2(x) + \psi_4 E_{o1}$ and $\psi_4 = \begin{bmatrix} h_{41} & h_{42} \\ h_{81} & h_{82} \end{bmatrix}$.

Then, the control law can be expressed as

$$A_{o0}(\hat{x})u + A_{o1}(\hat{x})\frac{du}{dt} = Z_o(t) \quad (22)$$

Where

$$Z_o(t) = C_{o0}(\hat{x})\varphi_3 \text{-} B_{o0}(\hat{x})\zeta \text{-} B_{o1}(\hat{x})\dot{\zeta} \quad (23)$$

With $A_{o0}(\hat{x})$, $A_{o1}(\hat{x})$, $C_{o0}(\hat{x})$, $B_{o0}(\hat{x})$ and $B_{o1}(\hat{x})$ are matrices.

Consider the observer given by equation by (10), with the CDM control specified by equation (22) and (23) and suppose that the gains δ and C_{o0} are such that

$$\left| C_{o0}\delta sign(Z_s)\int_0^t Z_4(\theta)d\theta \right| \ge |Z_3| + |H_o(\hat{x})| \quad (24)$$

After that, we establish the control signal that guaranties the asymptotic convergence of the error $Z_4(t)$.

The matrices are selected as follows

$$\begin{cases} A_{o0}(\hat{x}) = -K_o\left(dG_2(\hat{x})\right)/dt \\ A_{o1}(\hat{x}) = -K_o G_2(\hat{x}) \end{cases} \tag{25}$$

With $dG_2(\hat{x})/dt = diag(0,0)$, $K_o = diag(k_{o1}, k_{o2})$.

Where the element of K_o are positive constant.

After that, inserting equation (21) into (23) gives $Z_4 = (B_{o0}{}^{-1}C_{o0} - I)\varphi_3 - B_{o0}^{-1}Z_o$ and taking the matrix $C_{o0}(\hat{x}) = B_{o0}(\hat{x}) = C_{o0} = diag(c_{c1}, c_{c2})$ and placing $B_{o1}(\hat{x}) = diag(0,0)$ with $\delta = diag(\delta_1, \delta_2)$.

Then

$$Z_o = -C_{o0}Z_4 \tag{26}$$

After that, calculate the second derivative of Z_o as

$$\ddot{Z}_o(t) = C_{o0}\ddot{\varphi}_3(t) - C_{o0}\ddot{\zeta} \tag{27}$$

Inserting equation (22), (23) and employing (25) gives

$$\ddot{\zeta}(t) = \dot{G}_1(\hat{x}) + K_{o1}Z_o \tag{28}$$

With $K_{o1} = K_o^{-1}$, Substituting equation (27) and (28), result in $\ddot{Z}_o(t) = C_{o0}\ddot{\varphi}_3(t) - C_{o0}(\dot{G}_1(\hat{x}) + K_{o1}Z_o)$, then

$$\dot{Z}_o(t) = C_{o0}\dot{\varphi}_3(t) - C_{o0}(G_1(\hat{x}) + K_{o1}\int_0^t Z_o(\theta)d\theta) \tag{29}$$

Introducing equation (26) into (29) provides

$$\dot{Z}_4(t) = H_o(\hat{x}) - K_{o2}\int_0^t Z_4(\theta)d\theta \tag{30}$$

With $K_{o2} = C_{o0}K_{o1}$ and $H_o(\hat{x}) = G_1(\hat{x})\text{-}\dot{\varphi}_3(t)$, after that taking $K_{o2} = \delta sign(Z_s)$ and $Z_s = Z_4\int_0^t Z_4(\theta)d\theta$ gives

$$\dot{V}_4 = \dot{V}_3 + Z_4^T\dot{Z}_4 + \dot{V}_o \le -\bar{\lambda}_1 Z_1^T Z_1 - \bar{\lambda}_2 Z_2^T Z_2 - \bar{\lambda}_3 Z_3^T Z_3 + Z_3^T Z_4 + Z_4^T\dot{Z}_4 - \omega\left\|E_o\right\|^2$$

Therefore

$$\dot{V}_4 \le -\bar{\lambda}_1 Z_1^T Z_1 - \bar{\lambda}_2 Z_2^T Z_2 - \bar{\lambda}_3 Z_3^T Z_3 + Z_4^T(Z_3 + H_o(\hat{x}) - K_{o2}\int_0^t Z_4(\theta)d\theta) \tag{31}$$

As a result $\dot{V}_4 \le -\bar{\lambda}_1 Z_1^T Z_1 - \bar{\lambda}_2 Z_2^T Z_2 - \bar{\lambda}_3 Z_3^T Z_3 + v(t)$ Where $v(t) = Z_4^T(Z_3 + H_o(\hat{x}) - C_{o0}\delta Z_s sign(Z_s))$, if $v(t) < 0$, then the derivative of the final

Lyapunov function is $\dot{V}_4 \le -\bar{\lambda}_1 Z_1^T Z_1 - \bar{\lambda}_2 Z_2^T Z_2 - \bar{\lambda}_3 Z_3^T Z_3$. As a result $\dot{V}_4 \le 0$, this designates that the objective of angular positions control is finished.

5. PSO algorithm

PSO is a Bio-inspired evolutionary computation algorithm which is simple to implement for the reason that a few parameters should be tuned. The algorithm of PSO is implemented as follows. The unknown parameters are named the particles that construct the size of population. Beginning with a randomly initialization in positions and velocities in d_i dimensions where the solution exists. For each particle, evaluate its fitness function (MRSE). Then compare the MRSE of each particle with its best position. If current value is better than the previous best position, set the previous best position value to the current value and the previous best position among particles.

The evaluation of the velocity of i^{th} particle v_{ai} in the i^{th} iteration is given as (Zhong *et al.*, 2012).

$$v_{ai}\left(j+1\right) = \Gamma(v_{ai}(j) + c_{a1}r_1(p_{besti}(j) - p_{ai}(j)) + c_{a2}r_2(g_{best} - p_{ai}(j))) \tag{32}$$

Where $\left(r_1, r_2\right) \in \left[0 \quad 1\right]^2$, $\varepsilon = c_{a1} + c_{a2}$, $\varepsilon > 4$ and Γ is specified by (Gupta, 2015).

$$\Gamma = \frac{2}{\left|4 - \varepsilon - \sqrt{\varepsilon^2 - 4\varepsilon}\right|} \tag{33}$$

By using Γ, for any initial values of the particles, the PSO algorithm should discover the optimum solution.

For the i^{th} particle a new position is then calculated according to the following equations (Moharam *et al.*, 2016).

$$p_{ai}\left(j+1\right) = p_{ai}\left(j\right) + v_{ai}\left(j+1\right) \tag{34}$$

The PSO algorithm performs recurrently until the objective is attained. The number j_{max} can be set to a definite value as an objective of optimization.

MRSE is used throughout tuning parameters of controller. It is given for the i^{th} particle as follow

$$MRSE = \frac{1}{\mathbb{N}} \sum_{k=1}^{\mathbb{N}} \left(\sqrt{\sum_{k=1}^{4} \left\| Z_k(k) \right\|^2} \right) \tag{35}$$

The parameter values of PSO are chosen as follows d_i=23, s_p=120, $j_{max}=120$, c_{a1}=2.1, c_{a2}=2.1 and $r_1=r_2=0.71$.

Figure 3 shows a scheme to control the position of flexible robot using PSO.

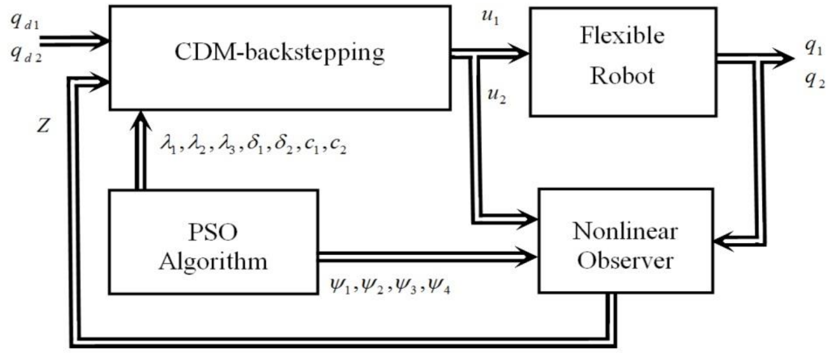

Figure 3. Block diagram of proposed control method

6. Simulation results

In order to demonstrate the feasibility, validity and effectiveness of the proposed controller, the simulation is carried out on the angular positions control of flexible manipulator, this system is supposed to follow a reference trajectory with the shape given in Figure 8 with the time span of 10s, while the mechanic parameters are in fact uncertain. The simulation result illustrated in Figure 4 to 13 shows the performance of the proposed control scheme, whose control objective is to ensure the asymptotic convergence of the tracking errors. Such simulation results reveal the performance comparison between conventional and optimized controllers. Purposely, the initial state is taken $x(0)=[0\ 0\ 0\ 0]^T$, where the observed initial state is chosen as $\hat{x}(0)=\left[\pi/4 \quad 0 \quad 0 \quad 0\right]^T$, which indicate that the observer error of the angular position has $\pi/4$ rad at $t=0s$. The nominal parameters of the concerned system are as follows: $m_1 = m_2 = 0.5\ kg$, $l_1 = l_2 = 0.3\ m$, $g = 9.8\ m/s^2$ $J_1 = J_2 = 0.1\ kg.m^2$, $K_{s_1} = K_{s_2} = 100\ N.m/rad$, $B_{a1} = B_{a_2} = 0.9\ N.m.s/rad$.

To have optimum performance, the gains of observer and controller are selected by the proposed method of optimization as given in Table 1.

6.1. Scenario 1

In the ideal case of numerical simulations, the initial errors are taken different to zero, not including any uncertainties, the controller performance is presented in Table 1 and Figure 4 to 9 and exposes the time angular positions of tracking for conventional and optimized controllers, from the results, It is concluded that the performance of the optimized controller is better than conventional controller in the transient responses without overshoot and or steady state error and assure still control efforts in the permitted values.

6.2. Scenario 2

To verify the robustness of the suggested controller, an external disturbance is applied and assumed as a sinusoidal function with a period of 5s and amplitude of *0.2 rad* inserted to the torque input, where the mechanic parameters are assumed to be 15% of uncertainties in length *L* and mass *M*, also, we introduce 6% of random noise in the measurements.

The simulation result for the reference in the presence of these uncertainties shows, respectively, the angular positions and controls inputs. As seen from Figure 9 to 13, the best performance obtained from the optimized controller in comparison to conventional controller appears in handling the external disturbances, uncertainties, as well, the effect of the noise on the positions, where the time responses converges asymptotically to zero with smaller settling times, without overshoots, with neglected steady state errors and by means of adequate controls effort. These results designate the effectiveness of the optimized controller.

Table 1. Comparison of algorithms performance

Algorithms	Parameters of control	$t_s(s)$	J
Conventional CDM-backstepping	$\left[\lambda_1,\lambda_2,\lambda_3,\delta_1,\delta_2.c_1,c_2\right]=$ $\left[8,7.5,7,112,100,0.65,0.75\right]$ $\psi_1=\begin{bmatrix}20 & 24\\ 21 & 17\end{bmatrix}$, $\psi_2=\begin{bmatrix}22 & 15\\ 35 & 16\end{bmatrix}$, $\psi_3=\begin{bmatrix}18 & 19\\ 33 & 22\end{bmatrix}$, $\psi_4=\begin{bmatrix}12 & 16\\ 34 & 13\end{bmatrix}$	$t_{s_1}=0.3$ $t_{s_2}=0.2$	13.0
PSO /CDM-backstepping	$\left[\lambda_1,\lambda_2,\lambda_3,\delta_1,\delta_2.c_1,c_2\right]=$ $\left[9.2,8.1,7,80,70,0.61,0.67\right]$ $\psi_1=\begin{bmatrix}15.1 & 18.0\\ 17.2 & 15.3\end{bmatrix}$, $\psi_2=\begin{bmatrix}17.2 & 13.1\\ 22.3 & 13.1\end{bmatrix}$, $\psi_3=\begin{bmatrix}16.2 & 14.1\\ 25.1 & 13.4\end{bmatrix}$, $\psi_4=\begin{bmatrix}10.1 & 12.0\\ 24.1 & 10.2\end{bmatrix}$	$t_{s_1}=0.1$ $t_{s_2}=0.1$	10.3

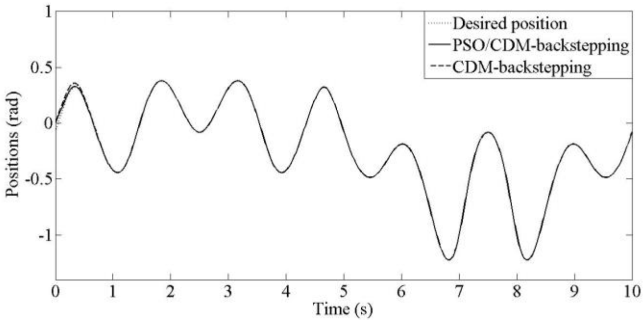

Figure 4. Positions of the first joint, Scenario 1

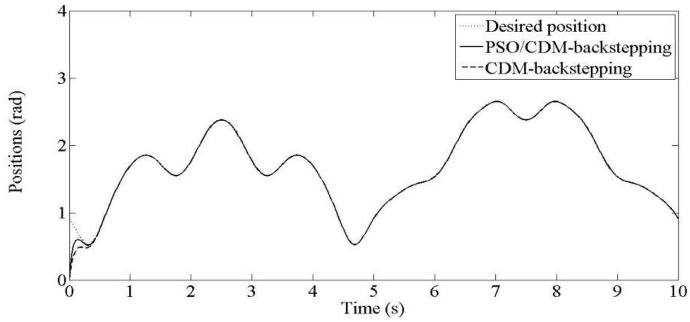

Figure 5. Positions of the second joint, Scenario 1

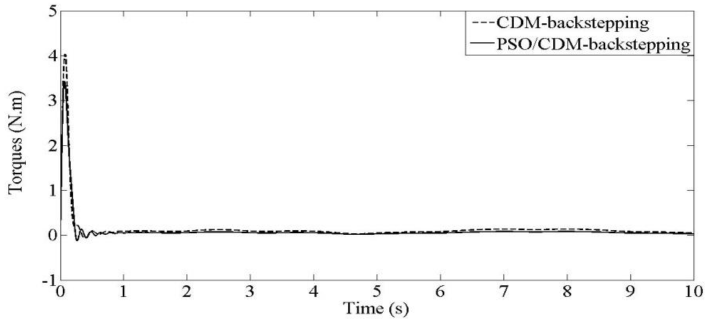

Figure 6. Torques of the first joint, Scenario 1

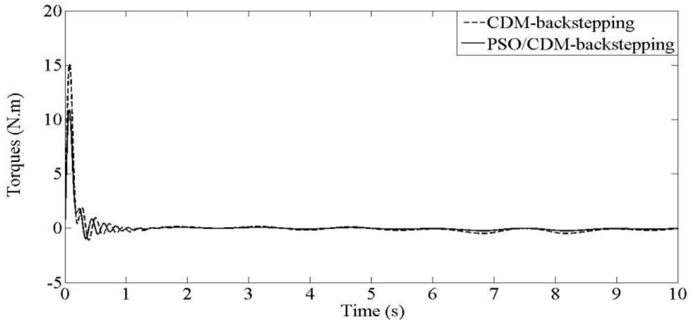

Figure 7. Torques of the second joint, Scenario 1

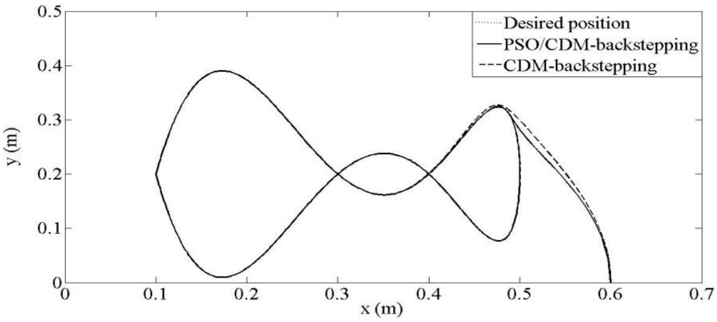

Figure 8. 2-D overview of tracking complicated trajectory, Scenario 1

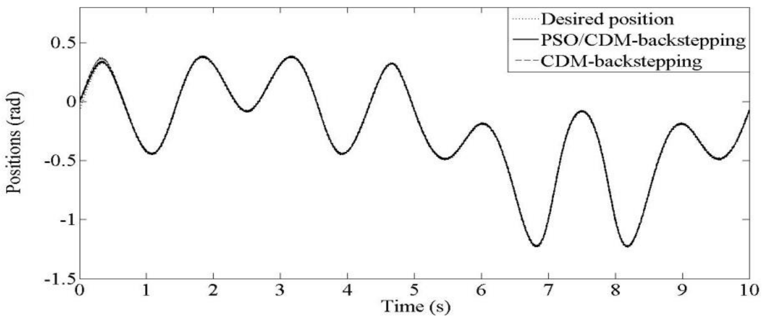

Figure 9. Positions of the first joint, Scenario 2

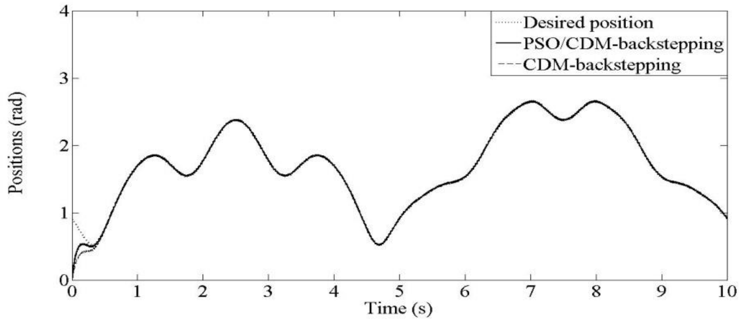

Figure 10. Positions of the second joint, Scenario 2

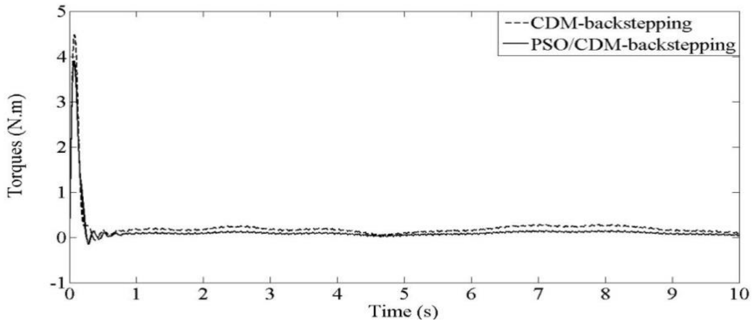

Figure 11. Torques of the first joint, Scenario 2

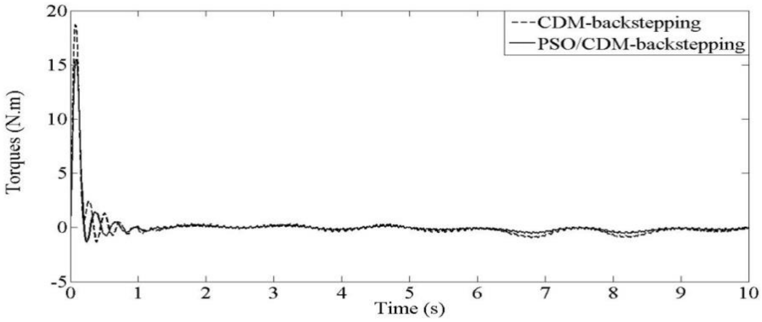

Figure 12. Torques of the second joint, Scenario 2

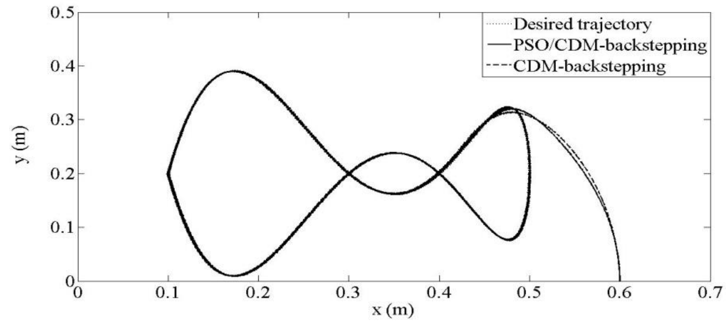

Figure 13. 2-D overview of tracking complicated trajectory, Scenario 2

7. Conclusion

In this paper, a nonlinear observer based on CDM-backstepping control was developed to control the angular positions of a two joints articulated flexible manipulator. The Lyapunov stability analysis was demonstrated to guaranties the asymptotic convergence of the trajectory tracking error of the entire system where the performance of the optimized controller using PSO was compared to the conventional controller.

In fact, parameters of the observer-controller were optimized to enhance the performance and increase the accuracy of control approach. In simulation results we observed using performance criteria such as MRSE, that the setting time reach to its minimum values without overshoot, and very suitable control effort that is confirmed to have more optimal values when compared with conventional controller.

References

Ali E. H., Karam E. H., Abbas H. A. (2014). Design and implementation of fuzzy PID controller for single link flexible joint robotic system using FPGA. *International Journal of Computer Applications*, Vol. 97, No. 7, pp. 26-33. Http://doi.org/10.5120/17020-7305

Ba D. X., Ahn K. K., Truong D. Q., Park H. G. (2016). Integrated model-based backstepping control for an electro-hydraulic system. *International Journal of Precision Engineering and Manufacturing*, Vol. 17, No. 5, pp. 565-577. https://doi.org/10.1007/s12541-016-0069-x

Benzineb O., Diallo D., Tadjine M., Benbouzid M. E. H. (2012). On fault-tolerant control of induction machines. An implicit approach. *European Journal of Electrical Engineering*, Vol. 15, No. 6, pp. 633-657.

Bernard M. Z., Mohamed T. H., Qudaih Y. S., Mitani Y. (2014). Decentralized load frequency control in an interconnected power system using coefficient diagram method. *Electrical Power and Energy Systems*, Vol. 63, pp. 165-172. https://doi.org/10.1016/j.ijepes.2014.05.057

Bossoufi B., Karim M., Lagrioui A., Taoussi M., Derouich A. (2015). Observer backstepping control of DFIG-Generators for wind turbines variable-speed: FPGA-based implementation. *Renewable Energy*, Vol. 81, pp. 903-917. https://doi.org/10.1016/j.renene.2015.04.013

Chang Y., Cheng C. C. (2010). Block backstepping control of multi-input nonlinear systems with mismatched perturbations for asymptotic stability. *International Journal of Control*, Vol. 83, No. 10, pp. 2028-2039. https://doi.org/10.1080/00207179.2010.501869

Chen F., Lei W., Zhang K., Tao G., Jiang B. (2016). A novel nonlinear resilient control for a quadrotor UAV via backstepping control and nonlinear disturbance observer. *Nonlinear Dynamic*, Vol. 85, pp. 1281-1295. https://doi.org/10.1007/s11071-016-2760-y

Furtat I. B., Tupichin E. A. (2016). Modified backstepping algorithm for nonlinear systems. *Automation and Remote Control,* Vol. 77, No. 9, pp. 1567-1578. https://doi.org/10.1134/S0005117916090058

Gupta I. K. (2015). A review on particle swarm optimization. *International Journal of Advanced Research in Computer Science and Software Engineering,* Vol. 5, No. 4, pp. 618-623. https://doi.org/10.1007/s40031-018-0323-y

Hassani K., Lee W. S. (2016). Multi-objective design of state feedback controllers using reinforced quantum-behaved particle swarm optimization. *Applied Soft Computing*, Vol. 41, pp. 66-76. https://doi.org/10.1016/j.asoc.2015.12.024

Khan I. U., Wagg D., Sims N. D. (2016). Nonlinear robust observer design using an invariant manifold approach. *Control Engineering Practice*, Vol. 55, pp. 69-79. https://doi.org/10.1016/j.conengprac.2016.06.015

Mitsantisuk C., Nandayapa M., Ohishi K., Katsura S. (2013). Design for sensorless force control of flexible robot by using resonance ratio control based on coefficient diagram method. *Automatika,* Vol. 54, No. 1, pp. 62-73. https://doi.org/10.7305/automatika.54-1.311

Mohamed T. H., Diab A. A. Z., Hussein M. M. (2015). Application of linear quadratic gaussian and coefficient diagram techniques to distributed load frequency control of power systems. *Applied Sciences*, Vol. 5, pp. 1603-1615.

Mohamed T. H., Shabib G., Ali H. (2016). Distributed load frequency control in an interconnected power system using ecological technique and coefficient diagram method. *Electrical Power and Energy Systems*, Vol. 82, pp. 496-507. https://doi.org/10.1016/j.ijepes.2016.04.023

Moharam A., El-Hosseini M. A., Ali H. A. (2016). Design of optimal PID controller using hybrid differential evolution and particle swarm optimization with an aging leader and challengers. *Applied Soft Computing*, Vol. 38, pp. 727-737. https://doi.org/10.1016/j.asoc.2015.10.041

Sabiri Z., Machkour N., Bezza M., Kheddioui E., Ouoba D. (2016). Non-linear command of wind turbine based on doubly-fed induction generator. *European Journal of Electrical Engineering*, Vol. 18, No. 5-6, pp. 385-397.

Wang J., He S., Lin D. (2016). Robust backstepping control for a class of nonlinear systems using generalized disturbance observer. *International Journal of Control Automation and Systems*, Vol. 14, No. 6, pp. 1475-1483. https://doi.org/10.1007/s12555-014-0401-0

Yen H. M., Li T. H. S., Chang Y. C. (2012). Adaptive neural network based tracking control for electrically driven flexible-joint robots without velocity measurements. *Computers and Mathematics with Applications,* Vol. 64, No. 5, pp. 1022-1032. https://doi.org/10.1016/j.camwa.2012.03.020

Yushu B., Zhihui G. (2013). Parameter optimization of controllable local degree of freedom for reducing vibration of flexible manipulator. *Chinese Journal of Aeronautics,* Vol. 26, No. 2, pp. 487-494. https://doi.org/10.1016/j.cja.2013.02.028

Zhong G., Kobayashi Y., Emaru T., Hoshino Y. (2012). Approaches based on particle swarm optimization for problems of vibration reduction of suspended mobile robot with a manipulator. *Journal of Vibration and Control,* Vol. 20, No. 1, pp. 3-23.

Zhou Q., Wu C., Jing X., Wang L. (2016). Adaptive fuzzy backstepping dynamic surface control for Nonlinear Input-delay systems. *Neurocomputing*, Vol. 199, pp. 58-65. https://doi.org/10.1016/j.neucom.2015.12.116

Nomenclature

q_1 : Link angle of the first joint

q_2 : Link angle of the second joint

$M(q)$: Generalized moment of inertia $C(q,\dot{q})\dot{q}$ is the centripetal and Coriolis forces

$G(q)$: Gravitational forces,

K_s : Matrix of joint stiffness coefficients

J : Motor inertia matrix

B_a : Actuator damping matrix

τ : Input torque

m_1 : Mass of the first link

m_2 : Mass of the second link

l_1 : Length of the first link

l_2 : Length of the second link

g : Gravity constant.

r_e : Reference input in CDM control

y_e : Output in CDM control

u_e : Control input in CDM control

e_r : Error signal in CDM control

d_e : External disturbance in CDM control

$N(s)$: Numerator of the system transfer function

$D(s)$: Denominator of the system transfer function

$A(s)$: Denominator polynomial of the controller

$B(s)$: Feedback numerator polynomials of the controller

$F(s)$: Pre-filter

$P(s)$: Characteristic polynomial of the closed loop system

μ_i : Coefficients of the characteristic polynomial

T_0 : Time constant

γ_i : Stability indices

γ_i^* : Stability limits

t_s : Settling time

κ : Constant Lipschitz.

ψ : Observer gain

E_o : Estimation error

P , Q : Symmetric positive definite matrices

ω, χ : Positive constants

Z_1 : First tracking error

E_{o1} : First estimation error

X_d : Vector of desired position

ψ_1 : First matrix gain

$\lambda_1, \lambda_2, \lambda_3, \overline{\lambda}_1, \overline{\lambda}_2, \overline{\lambda}_3, \kappa_1, \kappa_2, \kappa_3$: Positive constants

$\varphi_1, \varphi_2, \varphi_3$: Stabilizing control law

Z_2 : Second tracking error

E_{o2} : Second estimation error

ψ_2 : Second matrix gain

Z_3 : Third tracking error

E_{o3} : Third estimation error

ψ_3 : Third matrix gain

Z_4 : Fourth tracking error

E_{o3} : Fourth estimation error

ψ_3 : Fourth matrix gain

$h_{11}, \cdots, h_{82}$: Elements of matrix of observer gain

ζ : Auxiliary variable

$A_{o0}(\hat{x})$, $A_{o1}(\hat{x})$, $C_{o0}(\hat{x})$, $B_{o0}(\hat{x})$, $B_{o1}(\hat{x})$: Matrix of Nonlinear gains of Nonlinear CDM.

K_o, K_{o1}, K_{o2}, δ , C_{c0} : Diagonal matrix

c_{c1}, c_{c2} , k_{o1}, k_{o2} : Constants

d_i : Dimension of the problem space

p_{ai} : Position of the particle

p_{besti} : Previous best position of the particle

p_{best} : Previous global best position of particles
c_{a1} : Cognitive parameters
c_{a2} : Social scaling parameters
r_1 , r_2 : Pseudo-random numbers
ε : Constant
Γ : Constriction coefficient
j : Iteration number
j_{max} : Number of iterations
$MRSE$: Mean of root of squared error
$\mathbb{N}$: Number of samples errors.
s_p : Size of population
t_{s1} : settling time of the first position
t_{s2} : settling time of the second position